International Journal of Solids and Structures 236–237 (2022) 111265

Contents lists available at ScienceDirect

International Journal of Solids and Structures

journal homepage: www.elsevier.com/locate/ijsolstr

Novel non-linear static numerical model for curved masonry structures based on a combined adaptive limit analysis and discrete FE computations

Jacopo Scacco [a], Nicola Grillanda [a,*], Gabriele Milani [a], Paulo B. Lourenço [b]

[a] Department of Architecture, Built Environment and Construction Engineering (ABC), Politecnico di Milano, Piazza Leonardo da Vinci 32, 20133 Milan, Italy
[b] Department of Civil Engineering, ISISE, University of Minho, Azurém 4800-058, Guimarães, Portugal

ARTICLE INFO

Keywords:
Masonry vaults
Adaptive limit analysis
Automatic mesh generation
Discrete approach
Non-linear static analysis

ABSTRACT

A new procedure for a fast and comprehensive description of the collapse behavior of curved masonry structures is presented. The first step provides the identification of the exact collapse mechanism and the load-bearing capacity through adaptive NURBS limit analysis. This method is based on the discretization of the masonry vault through very few curved elements, assumed as rigid blocks with internal dissipation allowed only at interfaces, whose shape is iteratively modified until interfaces coincide with the correct position of cracks. On the obtained mechanism, a kinematic non-linear analysis with rigid-softening behavior can be also applied to better understand how the load-bearing capacity decreases during the evolution of the mechanism. A finite element (FE) non-linear static analysis is then applied to obtain the force–displacement curve according to the real elastic-softening behavior. The NURBS optimized model is converted into a discrete FE model composed of three-dimensional elastic units joint together by interfaces where the non-linear mechanical properties are lumped. Within this assumption, non-linear interfaces are applied along the cracks previously found through the limit analysis in a fully automatic way, preventing any mesh dependency effect. Furthermore, the combination of such approaches allows overcoming the respective drawbacks of the methods. Selected masonry arches and vaults are here studied to present the reliability of the presented coupled approach.

1. Introduction

Masonry vaults, arches and bridges are tangible evidence of the impressive skills and intuition of ancient builders. Such structures stand as distinctive elements of historical buildings such as churches, castles, palaces, and even housing aggregates which give significance to many European historical centers. Indeed, masonry structures play a fundamental role in cultural heritage and their structural preservation is nowadays crucial. As clearly established by ICOMOS guidelines, a correct intervention for the mitigation of vulnerability requires a comprehensive knowledge of the investigated structures. Correct understanding of the actual behavior can be reached by combining different approaches, involving historical investigation, non-destructive tests, and advanced computational analyses (Roca et al., 2010). Computational advanced approaches are particularly important to explore the ultimate behavior of such structures when subjected to loads not considered in their construction period. In particular, it is well known that curved structures are largely efficient only when gravity and, in general, vertical loads are considered. Still, a massive increase of such vertical loads (due for instance to a change of the intended use), asymmetrical loads, or the presence of soil settlements may promote the spreading of dangerous crack patterns (Portioli and Cascini, 2016; Iannuzzo et al., 2018; Fortunato et al., 2018; D'Altri et al., 2020; Zampieri et al., 2018; Zampieri et al., 2018; Zampieri et al., 2018). Full collapses are mainly related to extreme events such as earthquakes, explosions, or floods. In this context, the importance of developing efficient numerical tools for the analysis of curved masonry elements subjected to different load configurations is clear. As well known, the non-linear finite element approach is considered as the most powerful tool to carry out a wide range of analyses, from checks of the stress distribution under self-weight to more advanced simulations such as static and dynamic non-linear incremental analyses carried out with complex softening materials (Rossi et al., 2020). The level of complexity may become extremely high when a heterogeneous approach is used, see for instance (Calderón et al., 2019). As a matter of fact, the composite nature of masonry, made by mortar and bricks or stones assemblages, is accurately reproduced

* Corresponding author.
E-mail addresses: jacopo.scacco@polimi.it (J. Scacco), nicola.grillanda@polimi.it (N. Grillanda), gabriele.milani@polimi.it (G. Milani), pbl@civil.uminho.pt (P.B. Lourenço).

https://doi.org/10.1016/j.ijsolstr.2021.111265
Received 4 January 2021; Received in revised form 18 August 2021; Accepted 16 September 2021
Available online 16 October 2021

only by separately modeling each constituent material, but one of the main cons affecting detailed micro-modeling is related to the small thickness of mortar joints, which needs a high level of detail and the consequent use of a considerable number of finite elements for both joints and bricks, thus leading to a huge increase in terms of computational effort.

In this context, simplified micro-modeling can be adopted, where mortar thickness is neglected and assumed as an interface between adjoining blocks (Gaetani et al., 2020). A quite effective alternative can be found in a macro-modeling approach where masonry is substituted by a fictitious homogenous material (see for instance (Milani et al., 2009)). Such expedient is particularly useful when large-scale structures are analyzed and non-linear computations are carried out. Fictitious mechanical properties to be assigned to the homogenous material may be obtained in different ways, homogenization representing the most rigorous one. Homogenization can be carried out by means of several approaches, including FE-based methodologies (Rekik and Gasser, 2016) and semi-analytical ones (Bertolesi et al., 2016; Di Nino and Luongo, 2019). For instance, performing homogenization steps in the linear and non-linear range generally ensures a huge reduction of the complexity of the problem, without renouncing to a high level of accuracy (Krejčí et al., 2021).

Along with the finite element method (FEM), also discrete element methods (DEM) (Lemos, 2007) proved to be successful in specific fields of application, especially for masonry vaults and curved structures in general. In DEM, units interact mutually in correspondence with the interfaces, which typically follow a cohesive-frictional behavior. Unilateral contact and sliding in correspondence of the joints are accurately reproduced especially when dry joint masonry vaults are considered (for instance, successful 3-dimensional distinct element code 3DEC applications have been recently presented in (Foti et al., 2018; Sarhosis et al., 2019; Gobbin et al., 2020)). To the family of DEM approaches belongs also the so-called "RBSM" (Rigid Body and Spring Model), where interfaces are modeled with non-linear springs connecting rigid cells. Even though such a method proved to be sufficiently accurate, its application has been limited, in most cases, to separate in-plane (Casolo, 2004; Casolo and Peña, 2007; Milani and Bertolesi, 2017) or out-of-plane (Casolo and Uva, 2013; Silva et al., 2017; Bertolesi et al., 2019) loaded walls, given the intrinsic difficulty to keep rigorously coupled the membrane and flexural actions. Conversely, an automatic 3D discrete mesh generator for the non-linear analysis of curved masonry structures have been recently presented (Scacco et al., 2020). The method, validated by means of numerical and experimental comparisons, provided highly reliable and accurate results, while maintaining the computational burden under a certain threshold of acceptability. The great advantage of such a method was the concurrent reproduction of different features which are peculiar of masonry, like its orthotropic behavior and the influence of membrane normal stresses on the flexural behavior. In fact, the proposed method relies on an idealization of the structures constituted by the repetition of elastic cells connected by interfaces where all non-linearity has been concentrated. In particular, such interfaces have a finite thickness and are modeled with 8-noded brick elements. The softening behavior in the post-elastic phase is input through a classic Concrete Damage Plasticity (CDP) model available in the commercial code Abaqus, whose mechanical parameters are suitably tuned to account for the masonry orthotropy and softening behavior along different directions. This latter step is implemented as automatic kernel that allows performing direct numerical simulations. The discrete mesh is obtained automatically by means of an ad-hoc routine which transforms a standard 2D homogeneous FE mesh into a 3D orthotropic elastic model with interfaces where non-linearity is lumped. The orthotropy, preserved at each interface, can be automatically linked to different mechanical parameters according to its spatial orientation. Furthermore, the choice of modeling the structures with 3D elements is particularly suitable for curved surfaces, where the coupling between membrane and flexural actions plays a crucial role, that can be considered automatically only using a 3D discretization. On the other hand, such procedure may exhibit, as any discrete method, a certain mesh dependency. This is a consequence of the fact that non-linearities are exclusively lumped at the interfaces and a wrong estimation of the possible collapse mechanism in the first steps of the mesh creation, if suggested by user's intuition and not grounded on robust automatic procedures, might be responsible for inaccurate results.

The above-mentioned approach allows generally to fully track the evolution of cracks and displacements within a structure, fulfilling the requirements of advanced structural engineering. Even though approaches based on limit analyses do not provide any information on displacements, they proved to be able to effectively capture collapse mechanisms within a relatively narrow interval without being affected by mesh dependency, if the initial mesh is subjected to automatic adaptation. Such methodologies are modern applications of the classic limit analysis theorems, extensively applied by Heyman (Heyman, 1966; Heyman, 1969) for masonry arches.

A modern implementation of the static theorem of limit analysis applied to double curvature structures, known as Thrust Network Analysis (TNA), can be found in (Block and Ochsendorf, 2007; Block and Ochsendorf, 2008). However, even if the possibility to apply horizontal loads has been proven in (Marmo and Rosati, 2017; Marmo et al., 2019), the main application of such an approach is mainly focused on shape and material optimization for new dry joint structures (Adriaenssens et al., 2014). On the contrary, the latest implementations of the kinematic theorem revealed a versatility more oriented to studies related to earthquakes. In particular, some kinematic limit analysis tools based on an heterogeneous approach, i.e. with bricks and mortar modeled through rigid blocks and zero-thickness interfaces, have been presented during recent years (Portioli et al., 2014; Portioli et al., 2015; Cascini et al., 2020). In the field of masonry vaults, the first applications were carried out within classic FE formulations. An example is given by the use of rigid triangular six-noded elements enabling to fit satisfactorily the geometry of the vaults with few elements and with dissipation allowed only at the interfaces between contiguous triangles (Milani et al., 2008). On the other hand, if the mesh is not subjected to any adaptation scheme the solution remains mesh dependent. An attempt to circumvent such problem was tried initially by adjusting the mesh with Sequential Linear Programming (Milani and Lourenço, 2009; Milani, 2015), and subsequently by using few NURBS (Non-Uniform Rational B-Spline, (Piegl and Tiller, 1995) rigid elements with mesh adaptation. This latter approach guarantees fast computations, excellent fitting of the real geometry and independence from the initial mesh adopted. Mesh adaptation has been carried out first in (Chiozzi et al., 2017), combining NURBS with a genetic algorithm, and the procedure proved to be stable and to have a limited computational burden, at the same time allowing a correct identification of the ultimate load and the corresponding mechanism. Subsequently, the method has been further refined and applied to several typologies of masonry vaults. As mentioned before, the main limitation consists in the impossibility to track displacement and crack patterns evolution during the application of the loads. Moreover, it has to be mentioned that the assumption of a rigid-plastic behavior for masonry, which is one of the fundamental hypotheses of the upper bound limit analysis theorem, can lead to overestimations of the real load carrying capacity, even in presence of a correctly identified active collapse mechanism (as explained in (Corradi Dell'Acqua, 1994)). This effect is clearly visible when non-null values of tensile strength are adopted in the computations and the typical softening in tension is largely overestimated by means of the adoption of a perfectly plastic behavior. In these cases, an incremental procedure becomes fundamental for the correct estimation of the real load-bearing capacity of the structure.

The work proposed here is intended to provide an innovative coupling of the two aforementioned methodologies, in order to combine the successful features mentioned and tackle the respective drawbacks. Aiming at ensuring a limited computational burden, the discrete

approach proposed in (Scacco et al., 2020) is coupled with a previous kinematic adaptive limit analysis based on NURBS. In such a way, limit analysis is able to provide the correct collapse mechanism, which is automatically converted by the auto-meshing generator in Abaqus into a 3D discrete mesh. The initial user-made choice of the mesh is therefore irrelevant and non-linear analysis can be performed by less experienced users. Furthermore, in order to show the consistency of the two applied methods, a kinematic non-linear analysis, where the deformed shape of the structure is considered step-by-step, is implemented. This means that the collapse load (the upper bound in a kinematic analysis) is found for different deformed configurations up to the point in which equilibrium of the structure cannot be satisfied by limit geometric conditions.

The paper is organized as follows. In Section 2, the reliability of typical limit analysis outputs when the classic hypothesis of rigid-plastic behavior cannot be fulfilled is discussed. Section 3 contains a fully detailed explanation of the proposed coupled procedure. In Section 4, a range of structures of increasing complexity are studied and commented, including arches, skew arches, and a cloister vault. Finally, conclusions are drawn in Section 5.

2. Reliability of limit analysis for quasi-brittle materials

Consider a generic structure in the three-dimensional space $x_1x_2x_3$, whose volume and its outer boundary are indicated respectively by V and S. This structure is subjected to a pattern of volume loads $\{Q_0, \lambda Q\}$ and surface loads $\{q_0, \lambda q\}$, λ is a load multiplier applied to Q and q, and subscript 0 indicates the set of constant loads (e.g. gravity load in case of an earthquake load combination for which the maximum lateral load is sought). Consider an ideal rigid-plastic material, whose limit domain can be defined through M functions $f_\alpha(\sigma_{ij})$, $\alpha = 1,\dots M$, $i,j = 1, 2, 3$, in the stress space, the load multiplier is a static multiplier (λ_s) when an equilibrium configuration can be found with respect to plastic admissibility. In other words, the following conditions must be verified:

$$\begin{aligned} &\sigma_{ij,i} + Q_{0j} + \lambda_s Q_j = 0 \ \text{ in } \ V, \\ &\sigma_{ij} n_i = q_{0j} + \lambda_s q_j \ \ in\ S,\ \ i,j = 1,2,3 \\ &\sigma_{ij} n_i = q_{0j} + \lambda_s q_j \ \ in\ S,\ \ i,j = 1,2,3 \end{aligned} \tag{1}$$

where the equilibrium within the volume and along the outer boundary is expressed, and:

$$f_\alpha(\sigma_{ij}) \leqslant 0,\ \alpha = 1,\dots M,\ \ i,j = 1,2,3 \tag{2}$$

which represents the plastic admissibility.

Consider now a possible mechanism, defined by a discontinuous velocity field $\dot{u}$ with respect to an associative plastic flow rule, i.e. plastic velocities directed orthogonally to the limit domain, and such that the power dissipated by λQ and λq is positive. Discontinuities in the velocity field, indicated as $\Delta\dot{u}$, constitute the purely plastic deformations. The associative plastic flow rule is stated as follows:

$$\Delta\dot{u}_{ij} = \sum_{\alpha=1}^{M} \frac{\partial f_\alpha}{\partial \sigma_{ij}} \dot{p}_\alpha \ \text{ in } S, \ \ i,j = 1,2,3 \tag{3}$$

where $\dot{p}_\alpha \geq 0$ are the non-negative plastic multiplier rates. By applying the Principle of Virtual Power, a kinematic multiplier (λ_k) is identified:

$$\lambda_k \left(\int_V Q\dot{u}_j dV + \int_S q\dot{u}_j dS \right) + \int_V Q_0 \dot{u}_j dV + \int_S q_0 \dot{u}_j dS = \int_S \sigma_{ij} \Delta\dot{u}_{ij} dS \qquad i,j = 1,2,3 \tag{4}$$

where the right-hand side of Eq. (4) represents the internal dissipated power.

Under the hypotheses of small displacements, perfectly plastic behavior, and associative flow rule, the static and the kinematic theorem of limit analysis can be expressed, and the collapse multiplier (λ_c) can be identified as the minimum of the kinematic multipliers λ_k and the maximum of the static multipliers λ_s (Drucker et al., 1952):

$$\lambda_c = min(\lambda_k) = max(\lambda_s) \tag{5}$$

The collapse multiplier is not affected by the elastic properties, provided that deformability is limited, i.e. the collapse mechanism can occur with small displacements. Whatever approach is followed (static or kinematic), limit analysis allows to evaluate the peak load and the behavior at the collapse of the structure, provided that the previously mentioned hypotheses are verified. Otherwise, Eq. (5) is not valid and the failure evaluation can lead to partially inaccurate results. If limit analysis is used despite the lack of one of the fundamental hypotheses, the reliability of the result obtained must be checked on a case by case basis.

In particular, the hypothesis of perfectly plastic behavior of the material is the focus of attention here. Indeed, whereas this assumption is justified for steel, for masonry structures a different situation can be found. Limit analysis has been widely applied to curved masonry structures, such as arches and vaults (Heyman, 1966; Heyman, 1969; Como, 1992; Como, 2013). The assumption of infinitely rigid elements is justified for masonry, where the weak capacity to sustain tensile stresses usually leads to failures described through mutual rotations and translations of macro-blocks. A typical no-tension material is usually recommended for masonry, with a null value of limit stress in tension and the possibility to include failures in compression with respect to the hypothesis of perfect plasticity. However, exception made for dry-joints structures, the tensile strength of the mortar is usually low but not null (as shown during several experimental tests, see for instance (Hamid and Drysdale, 1988). Small values of tensile strength are often adopted in finite element incremental non-linear analyses (Scacco et al., 2020) and dynamic non-linear analyses with the aim of providing a more realistic representation of the structural behavior of masonry constructions and numerical convergence of the solutions. In these cases, an elastic-softening behavior with low fracture energy is assigned in tension.

When not-null tensile stress values are used within limit analysis procedures, perfectly plastic behavior is implicitly considered in tension. In reference to the kinematic theorem, the mechanism is associated with an internal dissipation which depends linearly on the jumps of velocity along the cracks (as indicated by the right-hand side of Eq. (4)). This is less realistic since the behavior of mortar is typically brittle in tension. When a crack occurs, its internal dissipation rapidly decreases to zero under small rotations, then the crack continues opening without dissipation. Therefore, it can occur that the maximum amount of internal power has been already dissipated along some fracture lines when the mechanism is completely developed, i.e. during the formation of the last crack needed for the mutual roto-translation of more blocks.

Within this context, it is clear that the internal dissipation evaluated as shown in Eq. (4) assumes a fictitious role when brittle behavior is involved, since it represents the amount of power that would be dissipated if the behavior were perfectly plastic. The rigid plastic behavior is the behavior that maximizes the load-bearing capacity of the analyzed structure. As a consequence, even if the correct collapse mechanism has been identified, the related kinematic load multiplier must be considered as a theoretical value which is an upper bound of the real collapse multiplier. If the mechanism takes place within the hypothesis of small displacements, the kinematic multiplier identifies a peak load equal to that found through incremental elastic–plastic analysis. Still, in presence of softening, the kinematic multiplier identifies a peak load that is higher than that obtained through incremental analysis with elastic-softening behavior (Corradi Dell'Acqua, 1994).

For a complete description of failure in presence of brittle behavior, incremental non-linear analyses with elastic-softening material and non-linearities in geometry are usually needed. Alternatively, an incremental rigid-plastic analysis in which the ultimate resistance values are progressively decreased during the opening of the cracks can be performed. This procedure mainly consists in the evaluation of the load-bearing capacity during the evolution of the mechanism. In this way, a

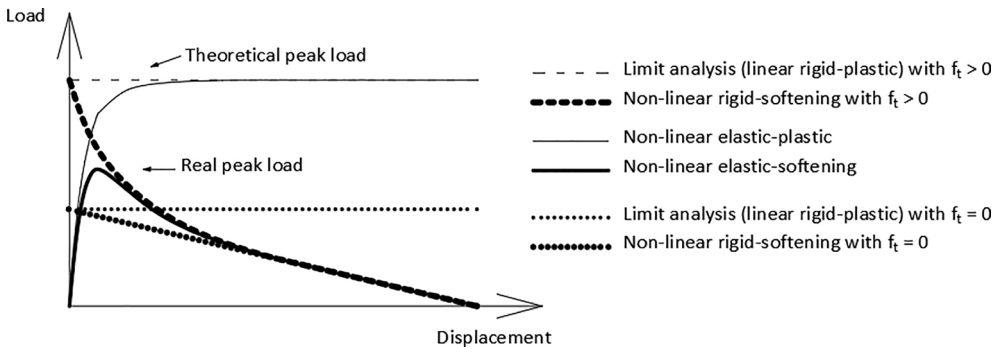

Fig. 1. Schematization of typical load–displacement diagram with different mechanical behaviors.

decreasing force–displacement curve is obtained, where displacement is referred to a control point and is representative of the evolution of the collapse mechanism. According to the previous considerations, this curve represents the upper bound of the peak load for each deformed configuration, which is described through the displacement of the control point from the undeformed configuration. Therefore, this rigid-softening curve will find higher load values than the non-linear elastic-softening force–displacement diagram as long as the structure is within the elastic field. Once the structure starts damaging and cracks occur, the two curves become tangent to each other.

A schematic representation of the force–displacement diagrams related to those different behaviors is depicted in Fig. 1, where the tensile stress f_t of masonry structures is used as the parameter representative of the softening behavior. The analogous linear rigid-plastic and non-linear rigid softening curves that would be found by using $f_t = 0$, i.e. the case with no internal dissipation, are shown for sake of completeness.

3. Proposed method combining limit analysis and non-linear finite element analysis

The main steps of the proposed approach are now described in detail. The first one consists of a kinematic limit analysis based on NURBS discretization and mesh adaptation. This first analysis is required to identify the maximum load-bearing capacity, i.e. the theoretical peak load under the hypothesis of ideal rigid-plastic material, and the correct shape of the failure mechanism. Once the collapse mechanism has been found, a kinematic non-linear analysis with softening in tension is also performed to determine how the load-bearing capacity decreases in each deformed configuration. The load–displacement curve for the rigid-softening material is obtained and taken into account as a reference for the final outcome. The next and final step is the FE incremental analysis with material and geometric non-linearities. This analysis is applied on a discrete model composed of elastic macro-blocks and non-linear interfaces located along the fracture lines previously identified through adaptive NURBS limit analysis. An elastic-softening load–displacement curve, which is an accurate representation of the real non-linear response of the structure, is found. The tangency between the rigid-softening and the elastic-softening curves must be observed in the numerical simulations.

3.1. Adaptive NURBS kinematic limit analysis

The first step of the proposed procedure is the adaptive NURBS kinematic limit analysis. This numerical technique was proposed as a reliable method for the limit analysis of masonry vaults (Chiozzi et al., 2017) and it has been extended to several typologies of masonry structures during recent years. This approach relies on the use of NURBS parametric surfaces for a faithful representation of curved geometries. A NURBS (Non-Uniform Rational B-Spline) surface is described by a set of control points in the three-dimensional space and the so-called NURBS basis functions, i.e. rational basis functions obtained from two non-uniform knot vectors and the traditional B-spline basis functions (Piegl and Tiller, 1995).

Within the Rhinoceros environment, a few surfaces can be used to represent the middle surface of a masonry vault (Fig. 2(a)). Then, the model is imported in MATLAB as an IGES file (Kennicott, 1996) where each surface is converted into a curved shell-element through the assignment of a thickness value. Within MATLAB, the subdivision of each NURBS surface into a low number of trimmed surfaces allows defining an initial mesh composed of a few elements which still maintains unaffected the geometry of the structure (Fig. 2(b)).

A kinematic limit analysis is then applied. Each element is supposed infinitely rigid and infinitely resistant. Curved interfaces are defined at the common boundaries between adjacent elements. Here, the internal dissipated power is evaluated by imposing a classical associated plastic flow rule depending on an assigned limit domain. With the aim of defining a limit domain with finite ultimate stress values, a Mohr-Coulomb three-dimensional failure domain with a tension cut-off and a linear cap in compression is used (Fig. 2(c), where f_t is the tensile strength, f_c is the compressive strength, c and φ are respectively the cohesion and the friction angle). This model also allows to assume not-null values of tensile strength within the hypothesis of rigid-plastic behavior. In addition, the typical orthotropic behavior of masonry can be reproduced by assigning two distinct limit domains (with the same shape but different resistance values) to the two main directions of each NURBS surface. Then, for each inclined interface, the two main domains are combined to provide the homogenized limit domain related to the direction of the current interface. Once a load-configuration $[\mathbf{q}_0, \lambda_k\mathbf{q}]$ (partially dependent on a load multiplier) is defined, the kinematic multiplier λ_k related to the initial mesh is derived by finding the vector of centroid velocities and plastic multiplier rates as $\mathbf{x} = [\dot{\mathbf{u}}, \dot{\mathbf{p}}]$ that solves the following linear programming (LP) problem:

$$min\left\{\lambda_k = \frac{\mathbf{c}\dot{\mathbf{p}} - \mathbf{q}_0\dot{\mathbf{u}}}{\mathbf{q}\dot{\mathbf{u}}}\right\} \text{ such that } \begin{cases} \mathbf{A}\dot{\mathbf{u}} = \mathbf{0} & (a) \\ \mathbf{R}\Delta\dot{\mathbf{u}} - \mathbf{B}\dot{\mathbf{p}} = \mathbf{0} & (b) \\ \mathbf{q}\dot{\mathbf{u}} = 1 & (c) \\ \dot{\mathbf{p}} \geqslant \mathbf{0} & (d) \end{cases} \tag{6}$$

where: (a) represents the geometric constraints, (b) is the imposition of the associated plastic flow rule at the interfaces (in which $\boldsymbol{\Delta}\dot{\mathbf{u}}$ are the jump of velocities and $\mathbf{R}$ is the matrix of the local reference systems), (c) is the normalization of the power dissipated by the base load $\mathbf{q}$ and (d) is the constraint of non-negativity of the plastic multiplier rates.

A mesh adaptation procedure aimed at minimizing the kinematic multiplier is now needed. Indeed, since the mechanism derived from Eq. (6) depends on the pre-assigned position of possible cracks, i.e. the initial mesh adopted, the collapse multiplier is determined by finding the mesh where the interfaces between elements correspond to the correct position of cracks. A Genetic Algorithm (GA) is thus used to iteratively modify the shape of elements until the absolute minimum of the kinematic multipliers is found. GA is one of the most suited approach

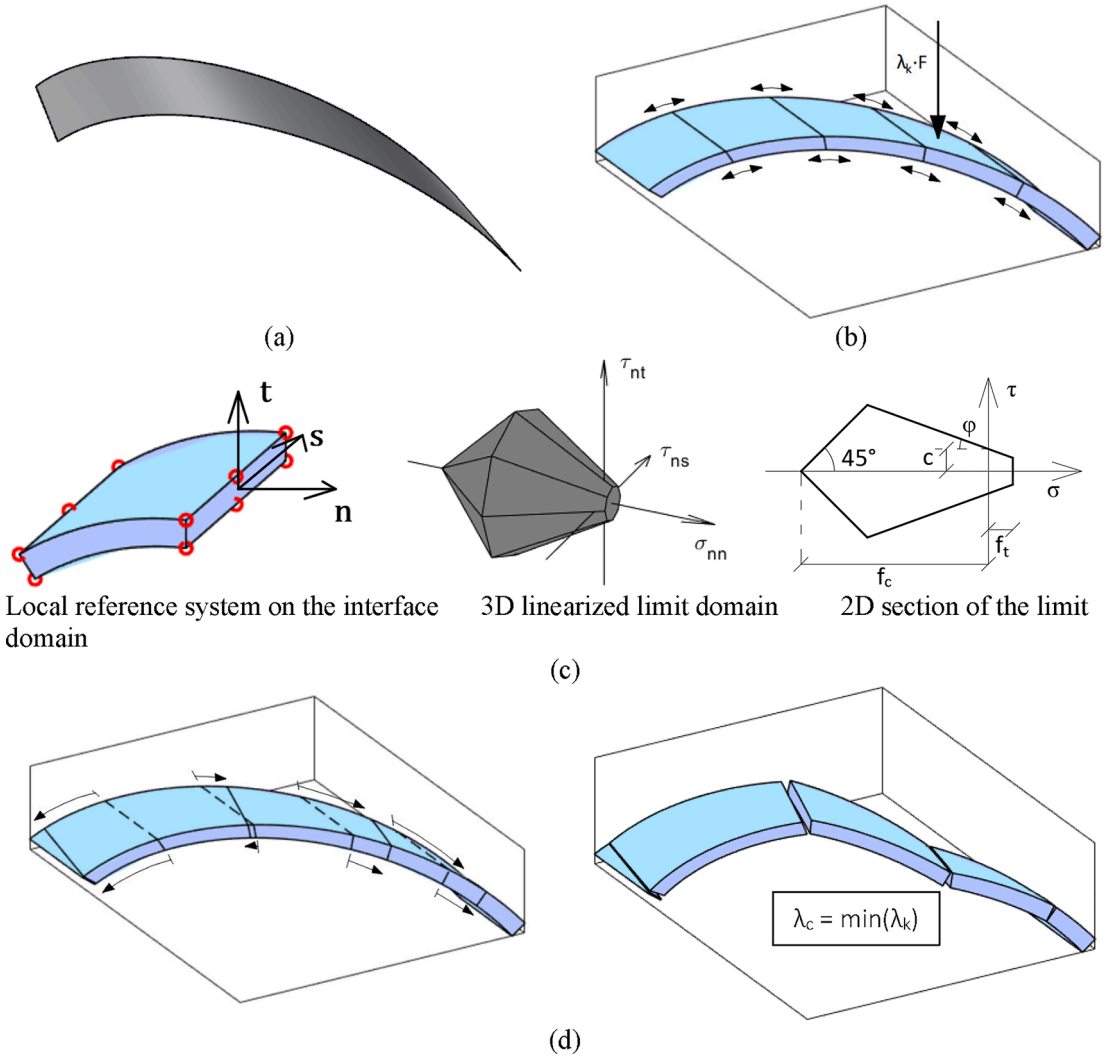

Fig. 2. Adaptive NURBS limit analysis: (a) NURBS surface representing a masonry skew arch, (b) NURBS model in MATLAB with adaptive mesh, (c) 3D limit stress domain at interfaces, and (d) result after the mesh adaptation.

for mesh adaptation schemes in masonry vaults (Milani, 2015; Ponterosso et al., 2000), even if other meta-heuristic algorithms can be successfully used within the adaptive NURBS limit analysis (Grillanda et al., 2020). At the end of this procedure, the collapse multiplier and the correct collapse mechanism have been automatically determined (Fig. 2 (d)).

The final mesh, optimized to reproduce the real position of cracks, can be easily exported from MATLAB again as an IGES file. This will be the input file for the discrete approach that will be described in the following sub-sections.

3.2. SLP kinematic non-linear analysis

Once the correct failure mechanism has been found, a procedure of kinematic non-linear analysis can be applied. According to the brief theoretical discussion presented in Section 2, this step is aimed at providing an upper bound load value for each deformed configuration until the equilibrium is no longer verified. Within this post-processing analysis, a load–displacement diagram which shows the dependence of the collapse load multiplier on the evolution of the mechanism is derived. For a reliable estimation of the structural capacity, a rigid-softening behavior in tension can be considered. An iterative procedure based on a Sequential Linear Programming (SLP) is here applied. At the first iteration, denoted as iteration 0, the initial geometry is updated by applying a displacement field $\mathbf{u}_0 = dt \cdot \dot{\mathbf{u}}_0$, where $\dot{\mathbf{u}}_0$ is the velocity field that identifies the collapse mechanism and dt is a small amount of time, allowing to treat $\mathbf{u}_0$ as a small displacement. A deformed configuration, where some of the cracks are partially open, is obtained in this way. At this point, if a rigid-softening behavior is considered in tension, the ultimate tensile strength values assigned to each interface must decrease. In particular, a lower tensile strength is assigned depending on a given stress–strain constitutive law and the amount of opening (i.e. the positive jump of displacement) measured on each interface. The LP problem is therefore re-written and solved in the deformed configuration, providing a new value of the collapse multiplier and a new discontinuous velocity field $\dot{\mathbf{u}}_1$. Another displacement field is obtained and a new iteration is performed. Ont the i-th iteration, the associated LP problem is the following (compare with Eq. (6)):

$$min\left\{\lambda_{c,i} = \frac{\mathbf{c}_{i-1}\dot{\mathbf{p}}_{i-1} - \mathbf{q}_0\dot{\mathbf{u}}_{i-1}}{\mathbf{q}\dot{\mathbf{u}}_{i-1}}\right\} \text{ such that } \begin{cases} \mathbf{A}_{i-1}\dot{\mathbf{u}}_{i-1} = \mathbf{0} & (a) \\ \mathbf{R}_{i-1}\Delta\dot{\mathbf{u}}_{i-1} - \mathbf{B}_{i-1}\dot{\mathbf{p}}_{i-1} = \mathbf{0} & (b) \\ \mathbf{q}\dot{\mathbf{u}}_{i-1} = 1 & (c) \\ \dot{\mathbf{p}}_{i-1} \geqslant \mathbf{0} & (d) \end{cases} \tag{7}$$

A load–displacement diagram is obtained, where the displacement is referred to a selected representative control point. A schematization example is depicted in Fig. 3. The iterative procedure goes on until a maximum displacement is reached, or in other words until the overall load configuration cannot be sustained anymore and the load-bearing

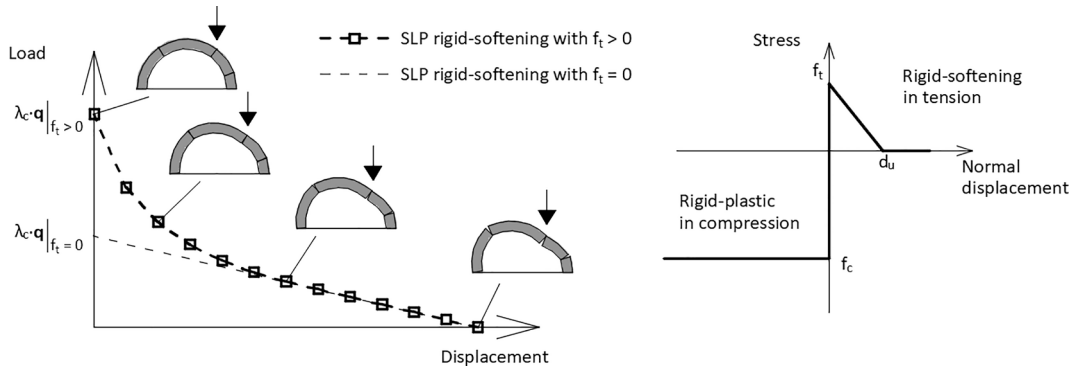

Fig. 3. Example of a kinematic non-linear analysis with rigid-softening behavior in tension.

capacity becomes null.

3.3. Automatic mesh generation for discrete FE non-linear analysis

The second step of the proposed method consists of a non-linear static analysis performed within the Abaqus FE software. The non-linear analysis here presented relies on an innovative discrete method already successfully validated for masonry plane elements (Scacco et al., 2020) and curved ones (Scacco et al., 2020). In such an approach, the masonry structure is idealized as an assembly of three-dimensional (3D) elastic units joined by interfaces where the non-linear mechanical properties are lumped. The properties may come directly from a previous homogenization procedure that allows to reduce significantly the global number of variables involved. Furthermore, such step can be based on semi-analytical approaches (further details can be found in (Scacco et al., 2020) as well) to avoid the performing of advanced and time consuming micro-modeling FE analysis at the Representative Volume Element (RVE) level.

At a structural level, which is the focus of the present work, the main innovation, which makes the method fast and attractive even from a practitioner point of view, is the way the non-linear interfaces are modeled. Indeed, flat 3D brick elements are used for this scope with a physical thickness that is considered negligible when compared to the overall dimension of the structure. The non-linear mechanical properties are addressed by means of the constitutive model Concrete Damage Plasticity (CDP) available in Abaqus. In particular, CDP is an isotropic elastic–plastic constitutive model with the possibility of damage (Lubliner et al., 1989). The shape of the yield surface follows the Drucker-Prager yield criterion, which can be modified to resemble smoothly a Mohr-Coulomb failure surface, more suitable when masonry-like materials are treated. Distinct behavior in tension and compression, with an exponential softening in tension and a hardening-parabolic softening in compression, are automatically provided within the CDP model.

As shown in (Scacco et al., 2020), the discrete approach showed great potential in the field of non-linear analysis of curved masonry structures. First of all, the idealization as a discrete assembly allows to address differential mechanical properties according to the interface orientation, preserving the orthotropy peculiar to masonry. Then, the choice of modeling the interfaces with 3D brick elements resulted to be highly appropriate, as it enables to take automatically into account the influence of membrane loads (coming from the static gravity actions) on the out-of-plane behavior. Moreover, the mesh discretization is made of a global number of nodes that is small when compared to advanced heterogeneous approaches. In such a way it is possible to perform non-linear analyses and track the evolution of inelastic behavior without unacceptably large computational time.

A possible drawback of the proposed approach may be found in the initial model preparation. Indeed, when curved elements are treated, the realization of a discrete mesh can result cumbersome and time-consuming when compared to other methods that take advantage of already implemented auto-mesh tools. Such possible difficulty is related to the choice, previously justified, of modeling interfaces with flat 3D brick elements. The physical thickness of these implies the necessity of ensuring gaps between the contiguous elastic discrete units. Aiming at a numerical tool easily employed even by less experienced users, a MATLAB script was implemented in (Scacco et al., 2020). The script is able to create automatically the final 3D discrete mesh starting from an initial definition of a rough mesh of the intrados of the curved structure considered. This step can be performed through a manually user-input

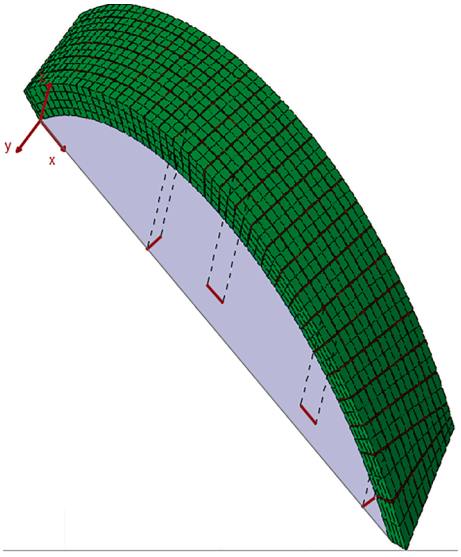

Fig. 5. Orientation of the non-linear interfaces in the skew arch benchmark.

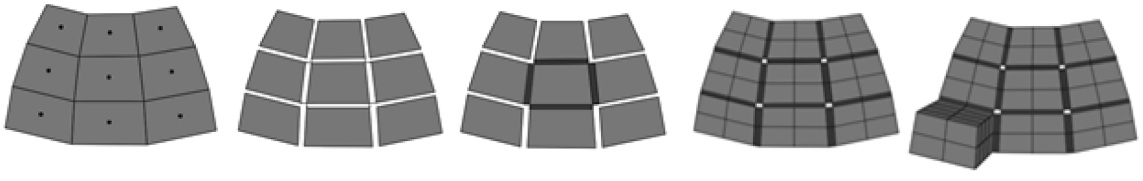

Fig. 4. Automatic creation of interfaces and 3D discretization.

or by means of any auto-meshing module already at the disposal in FE commercial software. From Fig. 4, which describes the auto-meshing procedure flow, it is noticeable that each 4-noded shell element of the mesh corresponds to one elastic 3D cell in the final discrete mesh with brick elements.

In fact, a shrinking operation (Fig. 4(b)) applied on each shell element allows to ensure the needed space for the subsequent creation of the interfaces. These are automatically generated as additional 4-noded thin elements, joining the contiguous elements (Fig. 4(c)). Then, each element is subdivided according to the desired discretization of the final 3D discrete model (Fig. 4(d)), which is finally obtained by a direct extrusion of the discrete shell mesh (Fig. 4(e)).

Furthermore, in presence of an orthotropic behavior, the script is able to assign automatically different mechanical properties to each interface according to its orientation in the space. If the available mechanical properties are referred to the vertical and horizontal directions, the program computes the tensile strength for any other direction I as follows:

$$\sigma_I = sin^2\theta \cdot \sigma_v + cos^2\theta \cdot \sigma_h \tag{8}$$

where σ_I, σ_v and σ_h are respectively the tensile strength of the interface under consideration and of the strength along the orthogonal directions (vertical and horizontally, typically); θ is the angle between the interface projections and the x-axis (a representative scheme is provided in Fig. 5).

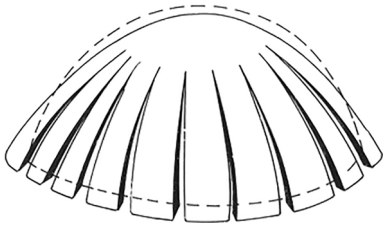

Fig. 6. Typical meridian cracks on masonry domes (Como, 2013).

3.4. Coupling

In (Scacco et al., 2020) the capabilities of the discrete method were highlighted and discussed in detail. Two different structural examples were analyzed taking advantage of already existing experimental and numerical references: a hemispherical dome and a cloister vault made of standard Italian bricks. Among other items, the past work focused on the influence of the initial mesh input and of the discretization applied. However, in those specific cases, the applied load is a simple vertical load at the top of the structures until failure. Such setup led to a damage configuration that may be trivial and easily foreseen by experienced users (see for instance the damage spreading along the meridians in the

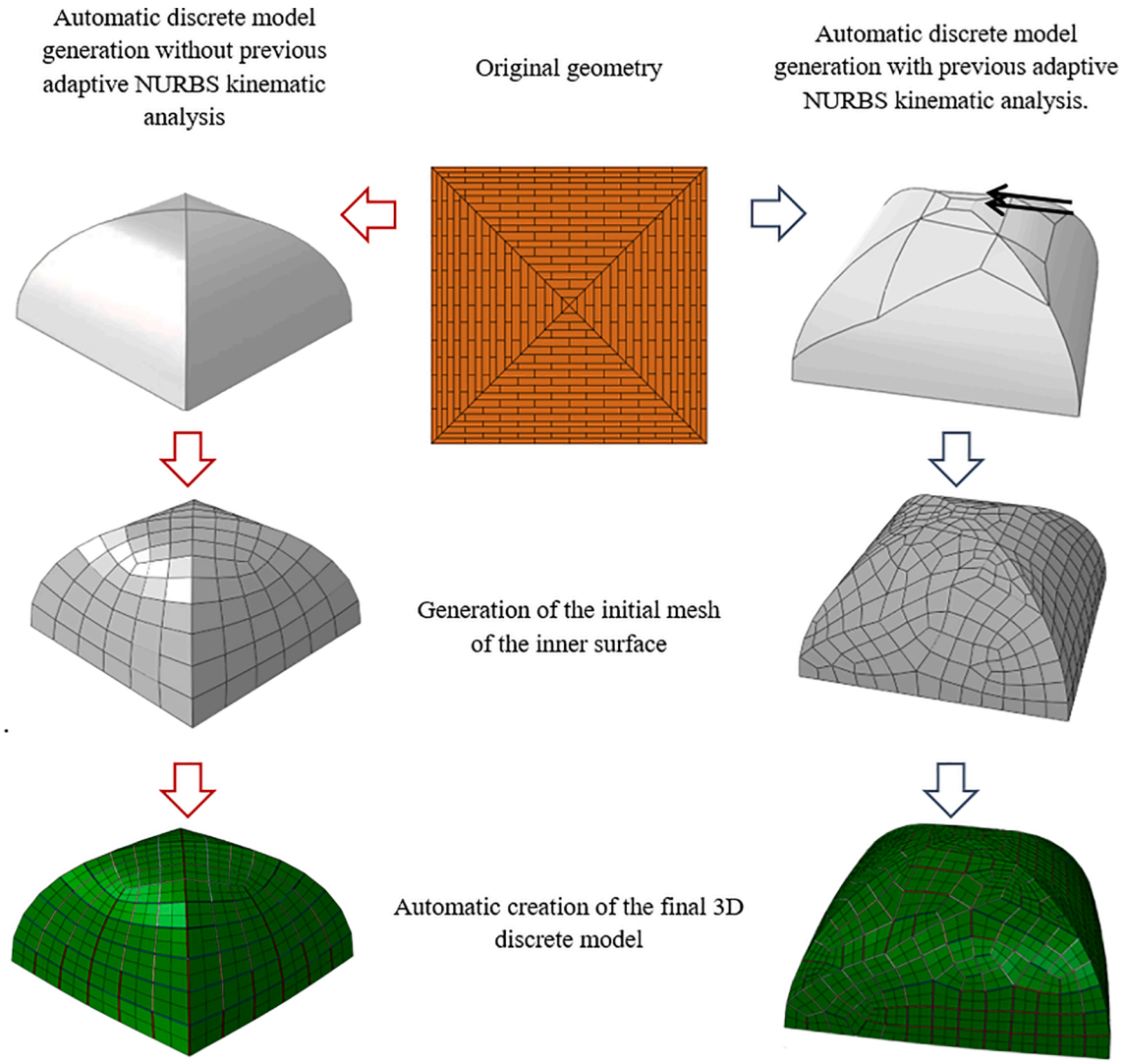

Fig. 7. Auto-meshing procedure without (left) and with (right) a previous kinematic analysis providing the collapse mechanism.

case of the dome as shown in Fig. 6). On the contrary, when the load cases are not covered in the literature, the initial input of the mesh of the inner surface may cause an overestimation of the capacity load and an inaccurate simulation of the collapse mechanism. Indeed, as any discrete approach, the proposed method can be affected by mesh dependency (Scacco et al., 2020) due to the arrangement and the size of the discrete units initially imposed.

In the present work, the main goal is the enhancement of the discrete approach by tackling the mesh dependency and finally providing a comprehensive method for the analysis of curved masonry structures. As non-linearities are concentrated only along the interfaces, there is the necessity to consider any possible important fracture lines during the initial mesh generation. In order to pursue this task, the adaptive NURBS kinematic limit analysis is adopted just before the flow-procedure of the automatic mesh generation to determine the exact shape of the collapse mechanism. The NURBS model and the derived optimized mesh are easily exported from MATLAB as an IGES file and then imported within Abaqus, where the discrete model is automatically generated. In such a way, the mesh of the inner surface is bounded not only by the geometry itself of the structure but also by the real fractures, detected through the adaptive NURBS limit analysis, along which the non-linear interfaces will be automatically created (Fig. 7). In the following analyses, the importance of adding such a step for extending the application field of the discrete approach to most complex structures and more varied load cases will be shown.

4. Numerical examples

Selected numerical examples are now presented as a demonstration of the potential of the proposed tools. For each example, the first step is the application of the adaptive NURBS limit analysis (LA) to define the correct shape of the collapse mechanism, identified by means of the optimized mesh, and an upper bound of the peak load evaluated within the hypothesis of perfect plastic behavior. The optimized mesh is then exported from MATLAB to Abaqus where the discrete approach (DA) can be applied. A discrete model with non-linear interfaces defined on the pre-obtained fracture lines is automatically generated. At this stage, a static non-linear analysis, in which both material and geometric non-linearities are taken into account, is performed by assigning elastic–-plastic behavior in compression and elastic-softening behavior in tension. A reliable force–displacement diagram is found in this way. For each case, the corresponding force–displacement curve with elastic–-plastic behavior in tension is also derived to better observe the analogy with this mechanical behavior and the rigid-plastic limit analysis. In addition, the previously described SLP-approach is also applied to derive the decreasing rigid-softening force–displacement curve that represents the variations of the upper bound of the peak loads during the evolution of the mechanism. Numerical examples include two masonry arches, one skew arch, and a cloister vault. For the sake of simplicity, Table 1 reports mechanical parameter values adopted for all examples.

4.1. Masonry arches

The analysis of simple two-dimensional masonry arches is beneficial to achieve awareness on the proposed superimposition of the two approaches before moving attention to complex double-curvature masonry vaults. With the aim of providing a more detailed overview on how softening in tension affects the collapse behavior, four values of tensile strength (from 0.05 MPa to 0.20 MPa, with steps of 0.05 MPa) were adopted for the masonry arches, together with different corresponding values of fracture energy. The other parameter values have been chosen consistently with (Bertolesi et al., 2016; Alecci et al., 2016), and, when missing, with typical values from technical literature.

Geometries and load conditions of the two examples are depicted in Fig. 8. The first masonry arch is a circular arch originally analyzed in (Bertolesi et al., 2016) through both experimental tests and numerical

Table 1
Masonry parameters adopted.

	Masonry arch #1	Masonry arch #2	Skew arch	Cloister vault
LA and SLP approach				
Specific weight γ	18 kN/m^3	18 kN/m^3	22 kN/m^3	20 kN/m^3
Tensile strength f_t	0.05 ÷ 0.20 MPa	0.05 ÷ 0.20 MPa	0.10 MPa	(1) 0.05 MPa (2) 0.09 MPa (*)
Ultimate displacement in tension d_u	0.2 mm	0.2 mm	0.2 mm	0.2 mm
Compression strength f_c	5 MPa	8 MPa	2.4 MPa	2.2 MPa
Cohesion c	0.20 MPa	0.20 MPa	0.14 MPa	0.1 MPa
Friction angle φ	0°	0°	30°	30°
DA				
Density ρ	1800 kg/m^3	1800 kg/m^3	2200 kg/m^3	2000 kg/m^3
Elastic modulus E	5000 MPa	5000 MPa	16000 MPa	1700 MPa
Poisson modulus ν	0.2	0.2	0.2	0.2
Tensile strength f_t	0.05 ÷ 0.20 MPa	0.05–0.20 MPa	0.10 MPa	(1) 0.05 MPa (2) 0.09 MPa (*)
Fracture energy in tension $G_f = f_t \cdot d_u/2$	0.005 ÷ 0.02 N/mm	0.005 ÷ 0.02 N/mm	0.01 N/mm	(1) 0.005 N/mm (2) 0.009 N/mm (*)
Compression strength f_c	5 MPa	8 MPa	2.4 MPa	2.2 MPa

(*) in which values (1) and (2) are adopted respectively for the failure along bed joints and orthogonal to bed joints

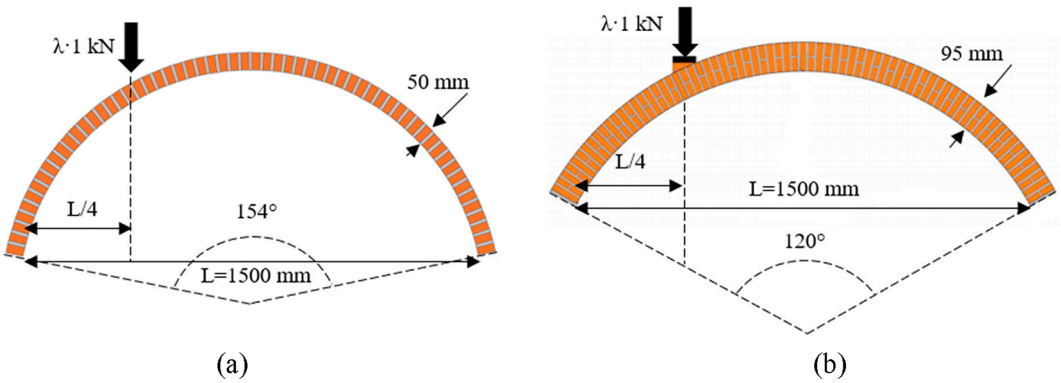

Fig. 8. Masonry arches (a) #1 (Bertolesi et al., 2016) and (b) #2 (Alecci et al., 2016): geometry and load condition.

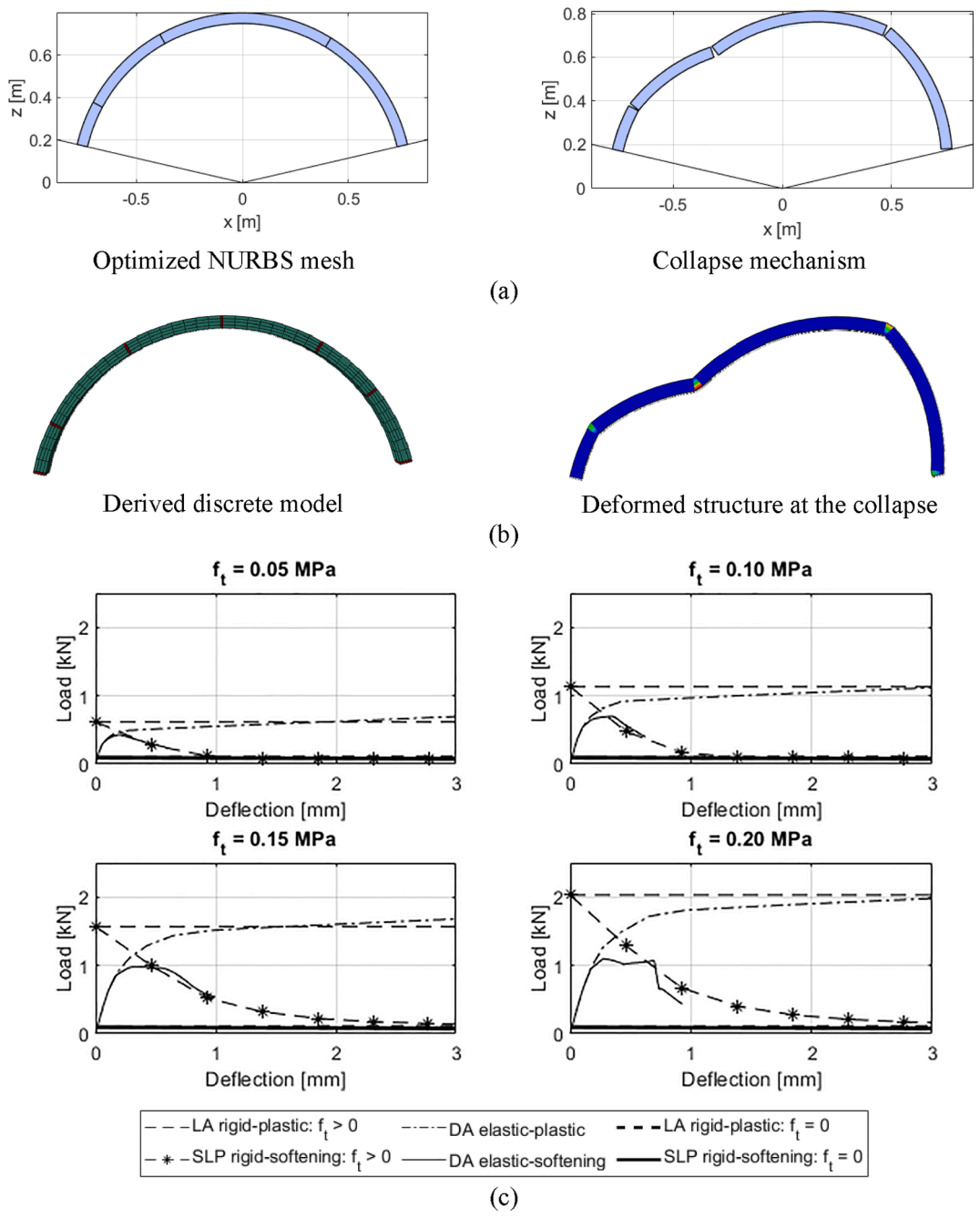

Fig. 9. Masonry arch #1: (a) optimized collapse mechanism, (b) deformed structure through the discrete approach, (c) force–displacement diagrams with different values of tensile strength and fracture energy.

analyses. This circular arch is characterized by an internal span of 1500 m, thickness of 50 mm, and width of 450 mm. The second arch, which was taken from (Alecci et al., 2016), is characterized by a geometry with internal span of 1500 mm, rise 432.5 mm, thickness and width both equal to 95 mm (see Fig. 8(b)). In both cases, a pointed vertical load is applied at a quarter of the span.

For both cases, the adaptive NURBS limit analysis has been used to find the exact position of the 3 internal hinges required for the definition of a mechanism (one hinge was supposed to occur in correspondence to one extremity of the arch). For the 3 hinge location parameters to be determined, a population of 20 individuals and a maximum of 100 generations have been used within the GA. Then, the optimized mesh

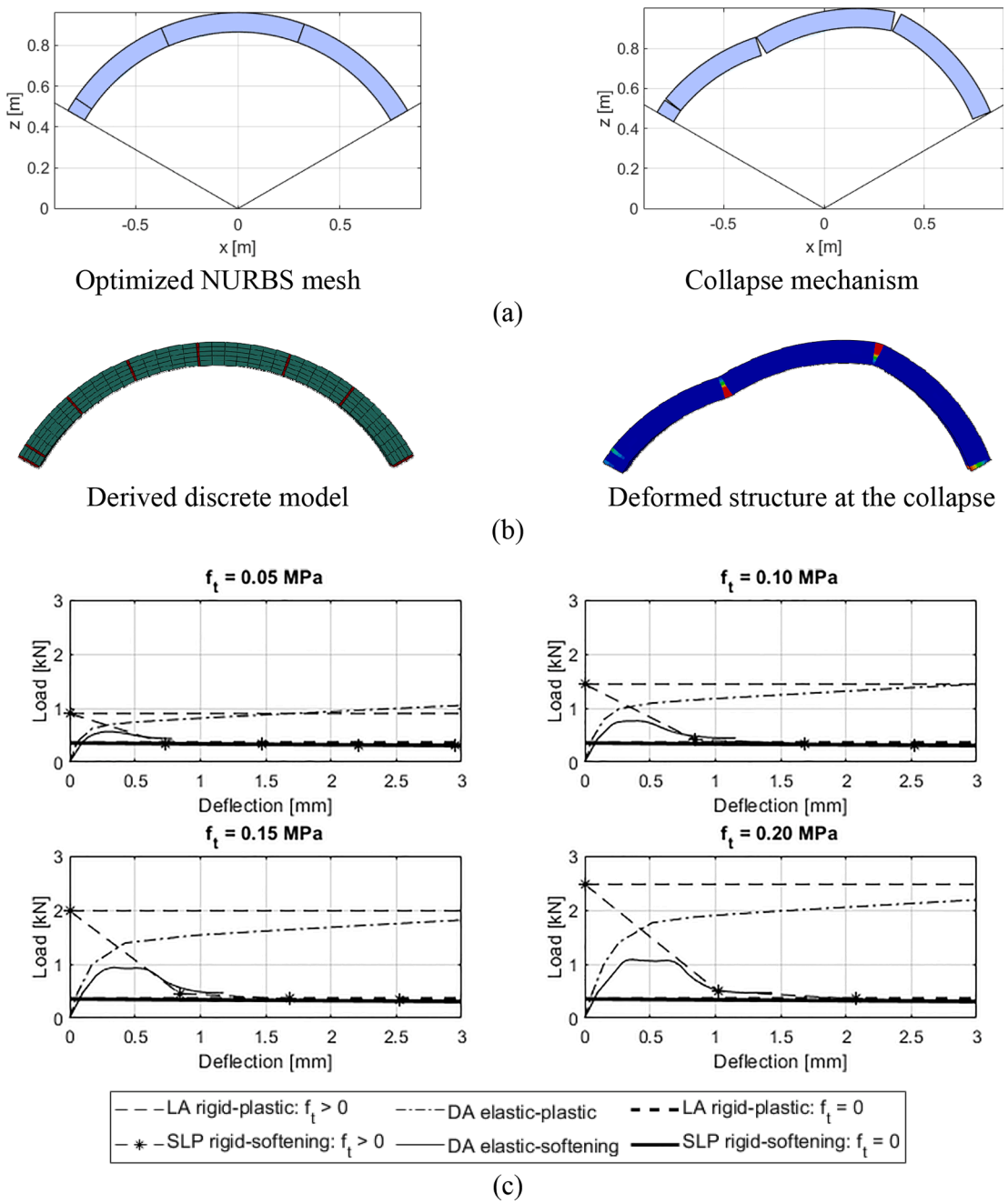

Fig. 10. Masonry arch #2: (a) optimized collapse mechanism, (b) deformed structure through the discrete approach, (c) force–displacement diagrams with different values of tensile strength and fracture energy.

has been imported within Abaqus as an IGES file to obtain the discrete model and perform static non-linear analyses through the presented discrete approach. Results are shown in Fig. 9 and Fig. 10 respectively for arch #1 and arch #2. It can be observed that a perfect agreement between the collapse shapes was found between the two models. In particular, Fig. 9(c) and Fig. 10(c) show the force–displacement diagrams corresponding to each value of tensile strength. As it can be observed, the discrete approach is the only tool able to correctly estimate the peak load especially in presence of a relatively high value of tensile strength, where the difference between the rigid-plastic and the elastic-softening peak load is clearly visible.

4.2. Skew arch

The transition from plane arches to skew arches is a fundamental step towards more complex cases. Indeed, even if the collapse mechanism generally involves the occurrence of four hinges (in the case of flexural behavior), the development of the fracture lines along the width can be difficult to predict without the support of a kinematic limit analysis. Therefore, a masonry skew arch first tested in (Wang and Melbourne, 1996) and analyzed in (Zhang et al., 2016) is considered next. The geometry is depicted in Fig. 11. This skew arch was studied also in (Chiozzi et al., 2017) and (Grillanda et al., 2020), where two circular hinges were applied at the extreme boundaries of the arch and a tensile strength equal to 0.2 MPa was used. In this work, to better reproduce the result obtained in (Zhang et al., 2016), the arch is fixed at the extreme boundaries and a tensile strength equal to 0.10 MPa is assigned (the same value used in (Zhang et al., 2016). Two different load cases have been here investigated, one already analyzed in (Chiozzi et al., 2017; Grillanda et al., 2020; Zhang et al., 2016), see Fig. 11.

Within the adaptive NURBS approach, the skew arch has been subdivided into 5 elements for both load cases. The four internal interfaces can move longitudinally and rotate around the vertical direction, resulting in a total of 8 parameters governing the mesh adaptation, to better represent the torsional effects due to the skew geometry. 40 individuals and 100 max generations have been used in the GA.

With reference to load case 1, the obtained result is presented in detail in Fig. 12. It can be observed that, starting from a load-bearing capacity of 26.65 kN obtained through limit analysis, the maximum peak load decreases to 18.47 kN after 1 mm of deflection. This is in good agreement with the numerical results presented in (Zhang et al., 2016). On this load case, the discrete approach has been applied by using also a non-optimized mesh to show the mesh-dependency of the method and thus to demonstrate the need to know the correct position of fracture lines. By using a regular non-optimized mesh, the maximum peak load is overestimated, see Fig. 13.

Finally, the analysis of skew arch under load case 2 is presented in Fig. 14. In this case, the load-bearing capacity is less affected by the softening in tension than the previous examples. Indeed, here the crushing of masonry assumes a fundamental role on each inclined hinge. As a consequence, the elastic-softening curve remains almost horizontal without decrease after a few millimeters of deflection.

4.3. Cloister vault

The last structural example considered treats the numerical simulation of a cloister vault. Like the previous cases, the geometry configuration (side 2 m, thickness 12 cm, Fig. 15) is taken from an existing experimental reference (Faccio et al., 1999), whereas the load case is specifically varied to accomplish the task of the paper. The discrete approach was already validated and the results were highly satisfactory for the case of the cloister vault subjected to a vertical load on the top (Scacco et al., 2020) (the experimental procedure in (Faccio et al., 1999). With the aim of inducing a more complex and hardly predictable damage pattern, the load case has been changed into a horizontal concentrated load applied at the top as depicted in Fig. 15. In this case,

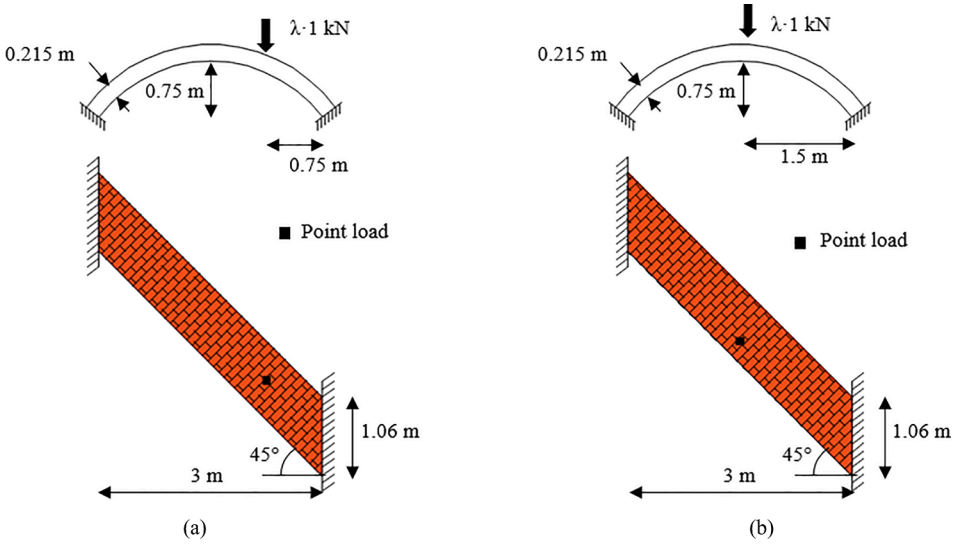

Fig. 11. Skew arch (Wang and Melbourne, 1996): geometry and load case (a) 1 and (b) 2.

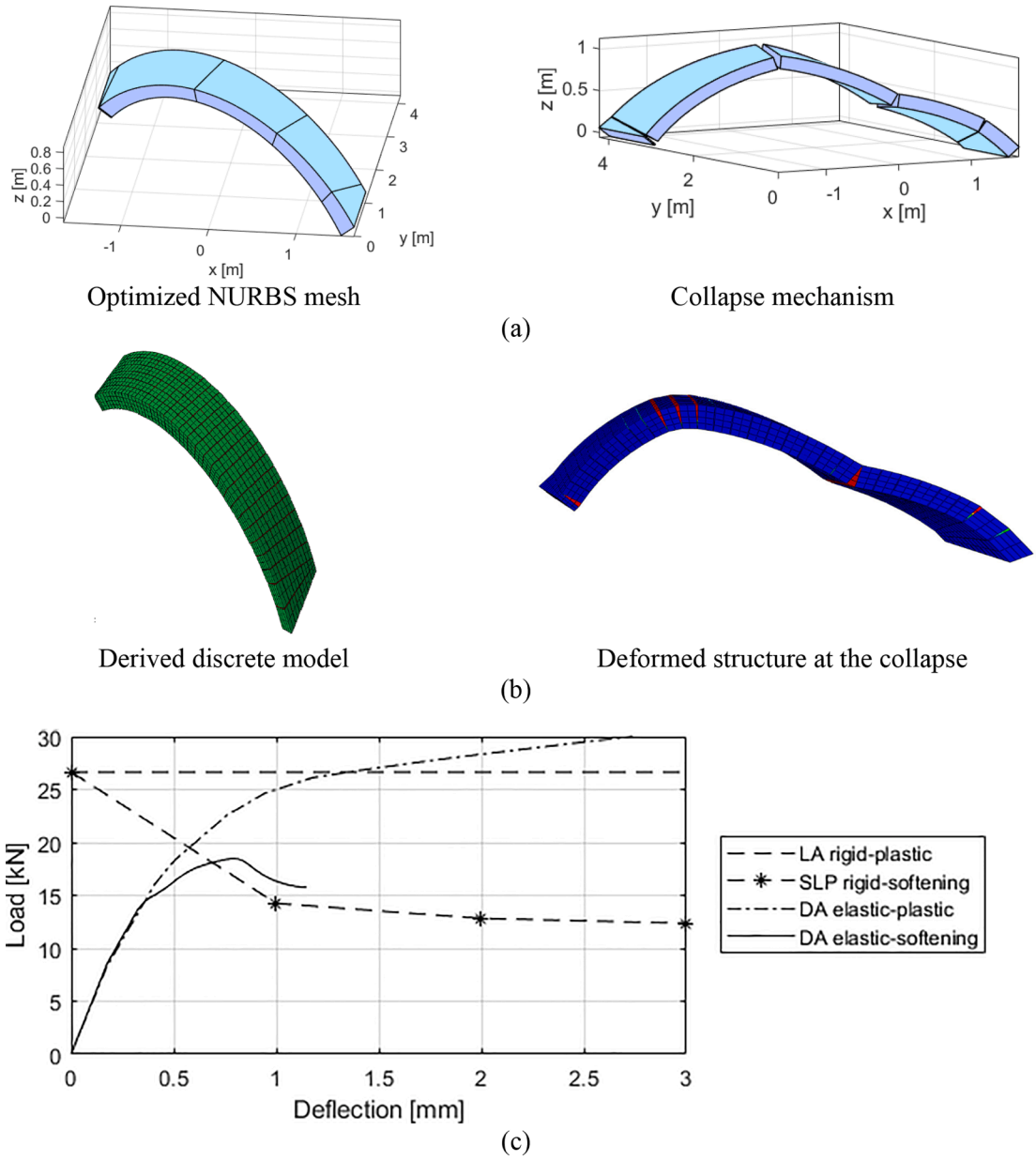

Fig. 12. Skew arch (Wang and Melbourne, 1996), load case 1: (a) optimized collapse mechanism, (b) deformed structure through the discrete approach, and (c) force–displacement diagrams.

an orthotropic behavior is assumed taking advantage of the already homogenized steps performed in (Scacco et al., 2020): in both the NURBS and the discrete model, two different values of tensile strength have been assigned along the vertical direction, i.e. failure on bed joints, and the horizontal one, i.e. orthogonal to bed joints. Isotropic behavior has been assumed in compression and shear.

Within the NURBS model, each sail has been subdivided into 7 curved macro-elements. The mesh adjustment of the single sail is governed by 10 parameters, each one representing a displacement of one internal knot (remember that knots located on a sail edge must move along the current edge) and thus resulting in a total amount of 32 parameters for the whole cloister vault. The symmetry of the problem in

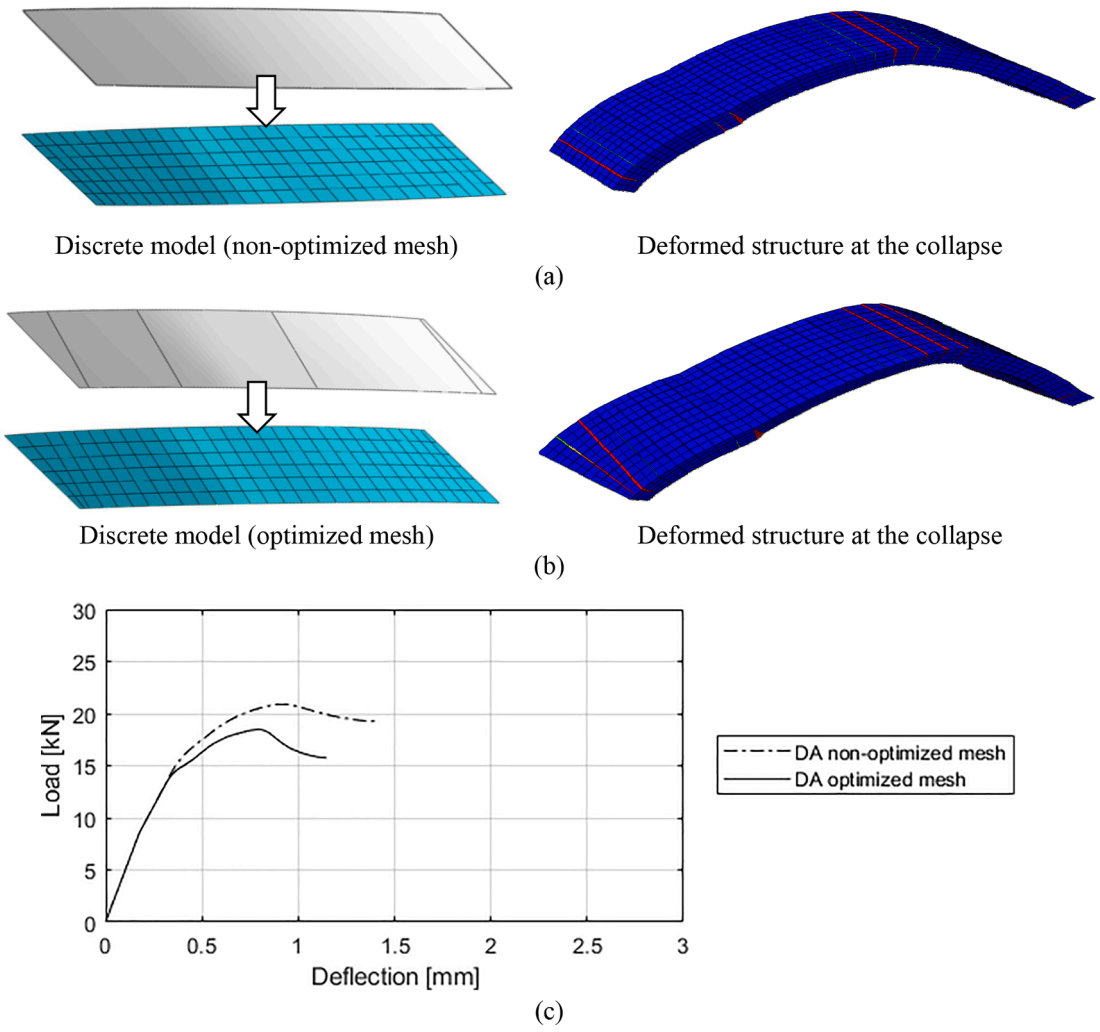

Fig. 13. Skew arch, load case 1, mesh-dependency of the discrete approach: result with (a) non-optimized and (b) optimized mesh, and (c) comparison between the two curves obtained.

terms of both geometry and load conditions allows us to reduce the number of parameters of the overall mesh adjustments to 16. A population size of 60 and a maximum generation number of 100 have been used within the GA. The collapse mechanism is depicted in Fig. 16(a). Fig. 16(b) shows the related discrete model. It has to be stated that, before exporting the IGES file from MATLAB to Abaqus, interfaces not involved in the mechanism (i.e. those characterized by null velocities jumps) have been removed to reduce the number of unknowns and the complexity of the discrete model. Even in this case, the deformed structure obtained through the DA is in good agreement with the mechanism previously found. This result is even more emphasized from the force–displacement diagrams presented in Fig. 16(c), where it can be seen that the DA elastic-softening merges perfectly the SLP rigid-softening after a horizontal displacement equal to 1 mm. In this last example is even more clear the effectiveness of the proposed coupled procedure, since LA is not able to properly identify the real peak load without further investigations.

5. Conclusions

In this paper, an innovative coupled procedure for the non-linear analysis of curved masonry structures has been presented. First, the

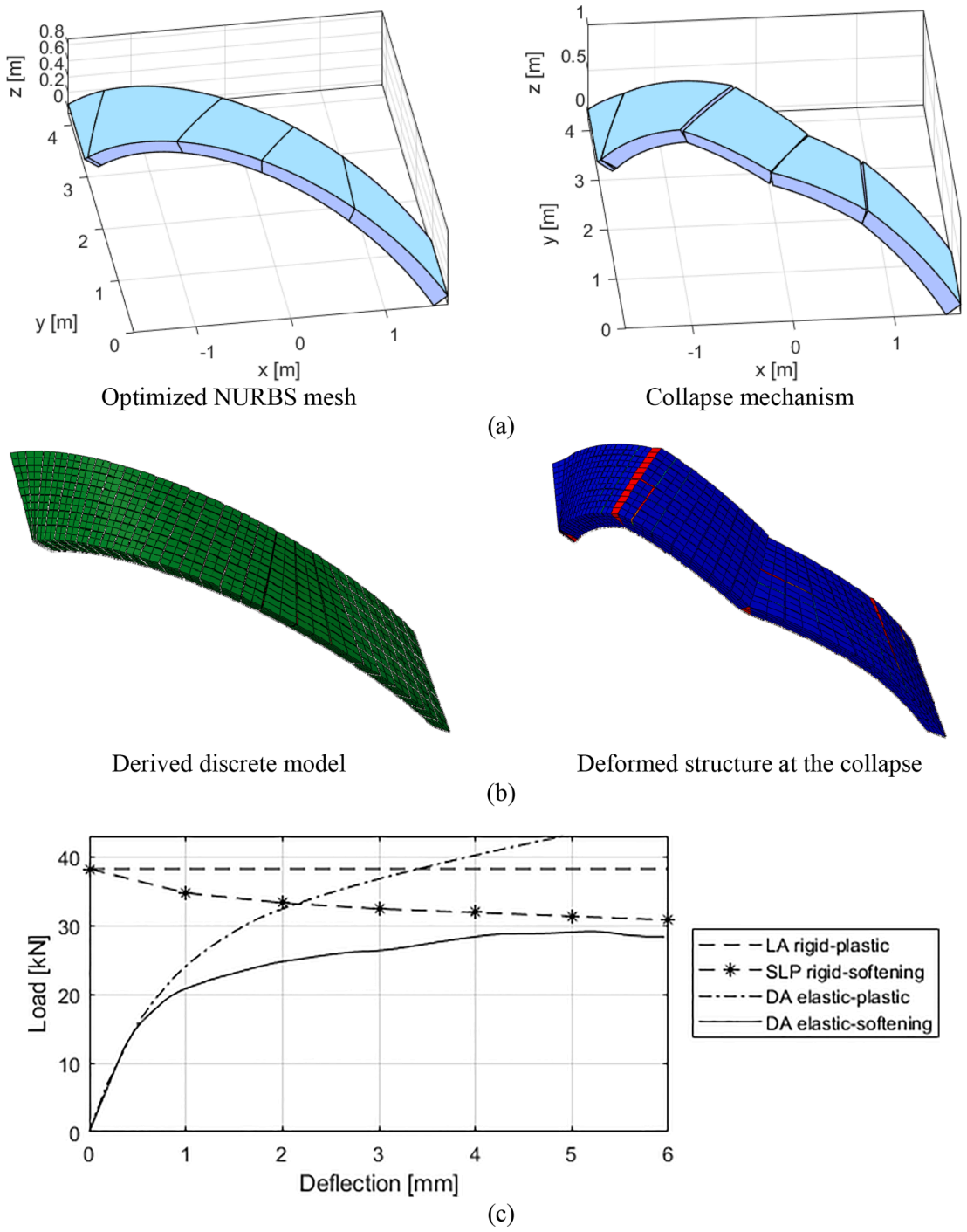

Fig. 14. Skew arch (Wang and Melbourne, 1996), load case 2: (a) optimized collapse mechanism, (b) deformed structure through the discrete approach, and (c) force–displacement diagrams.

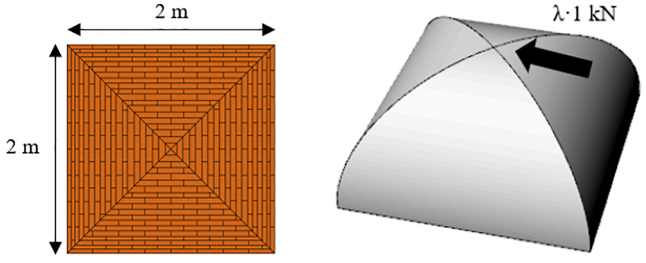

Fig. 15. Cloister vault (Faccio et al., 1999): geometry and load conditions.

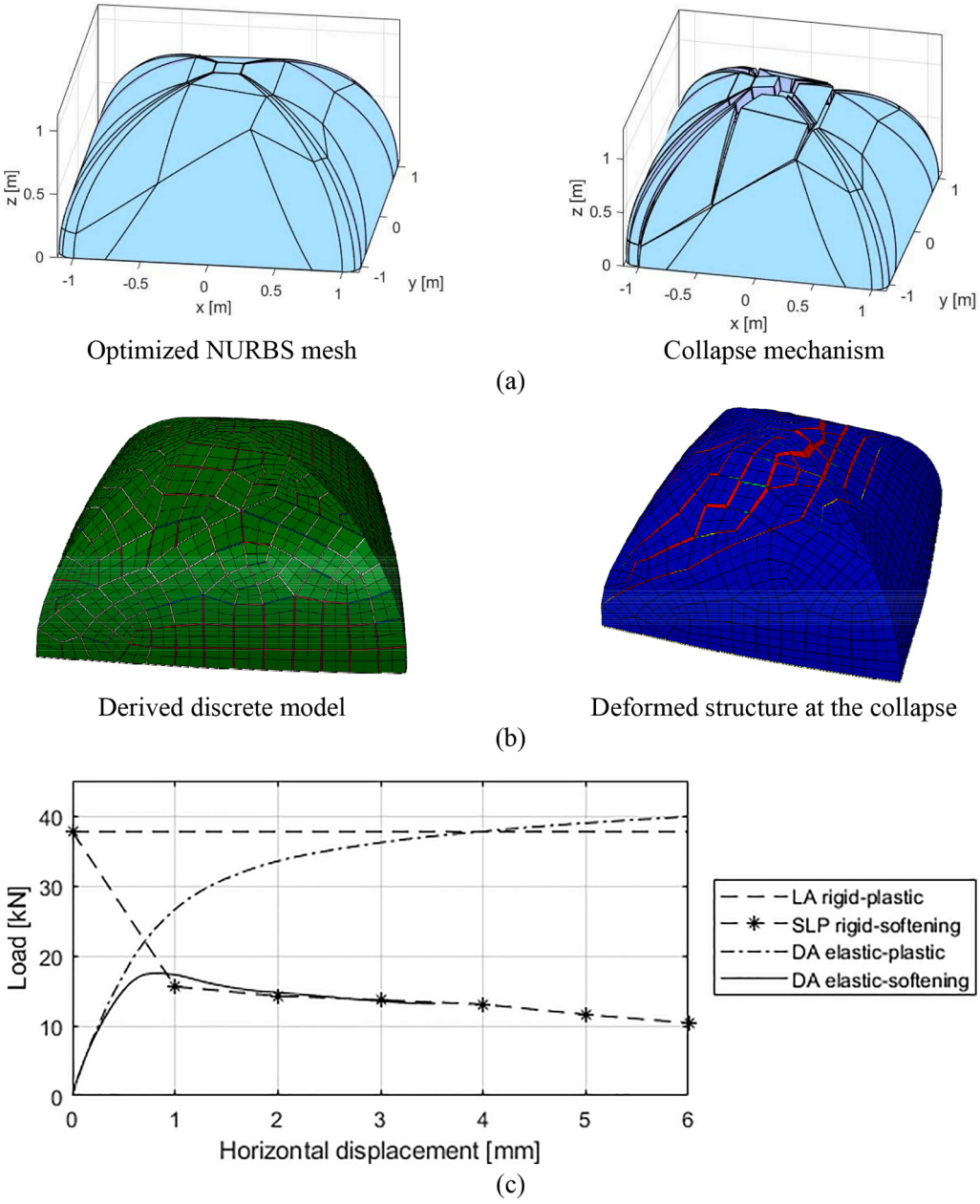

Fig. 16. Cloister vault under horizontal load: (a) optimized collapse mechanism, (b) deformed structure through the discrete approach, and (c) force–displacement diagrams.

collapse mechanism has been defined through a consolidated adaptive NURBS limit analysis approach, which allows to find the real position of fracture lines with a low computational cost. With the obtained result, a discrete FE mesh has been automatically created through totally integrated kernel subroutines and non-linear analyses have been performed directly interfacing with limit analysis and mechanical properties coming from homogenization or other suitable approaches. The automatic conversion of the rigid curved NURBS macro-blocks into 3D elastic elements with non-linear interfaces allows to carry out fast pushdown or pushover analyses, avoiding any overestimation due to wrong initial inputs on the initial mesh. In such a way, the proposed coupled procedure is able to balance the well know intrinsic disadvantages of both methods when independently applied. Along with the main two steps (limit analysis and elastic-softening analysis), kinematic rigid-softening and elastic–plastic analyses have been used to enforce the reliability of the results obtained, providing a further validation and presenting in parallel comparison of the structural response under the assumption of different mechanical behaviors. Several numerical examples have been investigated, such as simple masonry arches, skew arches, and a horizontally loaded cloister vault. In all cases considered, the proposed method allowed to correctly derive the expected global load–displacement non-linear behavior, according to the existing literature used as benchmark. Moreover, the mesh dependency of the discrete approach (step 2) has been investigated using as main benchmark the skew arch case; the results obtained have shown how the adaptive limit analysis (step 1) appears crucial for the determination of the actual position of the cracks spreading during the loading process. In conclusion, coupling adaptive limit analysis with a discrete approach may result to be an effective numerical strategy for obtaining a fast and comprehensive understanding of the non-linear behavior up to collapse behavior of curved masonry structures modeled with a material exhibiting softening and orthotropy.

Declaration of Competing Interest

The authors declare that they have no known competing financial interests or personal relationships that could have appeared to influence the work reported in this paper.

References

Adriaenssens, S., Block, P., Veenendaal, D., Williams, C., 2014. Shell Structures for Architecture Form Finding and Optimization. Routledge, London.

Alecci, V., Misseri, G., Rovero, L., Stipo, G., De Stefano, M., Feo, L., Luciano, R., 2016. Experimental investigation on masonry arches strengthened with PBO-FRCM composite. Compos. B Eng. 100, 228–239.

Bertolesi, E., Milani, G., Lourenço, P.B., 2016. Implementation and validation of a total displacement non-linear homogenization approach for in-plane loaded masonry. Comput. Struct. 176, 13–33.

Bertolesi, E., Milani, G., Fedele, R., 2016. Fast and reliable non-linear heterogeneous FE approach for the analysis of FRP-reinforced masonry arches. Compos. B Eng. 88, 189–200.

Bertolesi, E., Silva, L.C., Milani, G., 2019. Validation of a two-step simplified compatible homogenisation approach extended to out-plane loaded masonries. Int. J. Masonry Res. Innovat. 4, 265–296.

Block, P., Ochsendorf, J., 2008. Lower-bound analysis of masonry vaults, in: Structural Analysis of Historic Construction. Taylor & Francis Group, London.

Block, P., Ochsendorf, J., 2007. Thrust network analysis: A new methodology for three-dimensional equilibrium. J. Int. Assoc. Shell Spat. Struct. 48, 1–7.

Calderón, S., Arnau, O., Sandoval, C., 2019. Detailed micro-modeling approach and solution strategy for laterally loaded reinforced masonry shear walls. Eng. Struct. 201, 109786.

Cascini, L., Gagliardo, R., Portioli, F., 2020. LiABlock_3D: a software tool for collapse mechanism analysis of historic masonry structures. Int. J. Architect. Herit. 14 (1), 75–94.

Casolo, S., 2004. Modelling in-plane micro-structure of masonry walls by rigid elements. Int. J. Solids Struct. 41, 3625–3641.

Casolo, S., Peña, F., 2007. Rigid element model for in-plane dynamics of masonry walls considering hysteretic behaviour and damage. Earthquake Eng. Struct. Dyn. 36, 1029–1048.

Casolo, S., Uva, G., 2013. Nonlinear analysis of out-of-plane masonry façades: full dynamic versus pushover methods by rigid body and spring model. Earthquake Eng. Struct. Dyn. 42, 499–521.

Chiozzi, A., Milani, G., Tralli, A., 2017. A Genetic Algorithm NURBS-based new approach for fast kinematic limit analysis of masonry vaults. Comput. Struct. 182, 187–204.

Como, M., 1992. Equilibrium and collapse analysis of masonry bodies. Meccanica 27, 185–194.

Como, M., 2013. Statics of Historic Masonry Constructions. Springer Berlin Heidelberg, Berlin, Heidelberg.

Corradi Dell'Acqua, L. 1994. Meccanica delle strutture - La valutazione della capacità portante, McGraw-Hill, Milano (In Italian).

D'Altri, A.M., De Miranda, S., Castellazzi, G., Sarhosis, V., Hudson, J., Theodossopoulos, D., 2020. Historic Barrel Vaults Undergoing Differential Settlements. Int. J. Architect. Herit. 14 (8), 1196–1209.

Di Nino, S., Luongo, A., 2019. A simple homogenized orthotropic model for in-plane analysis of regular masonry walls. Int. J. Solids Struct. 167, 156–169.

Drucker, D.C., Prager, W., Greenberg, H.J., 1952. Extended limit design theorems for continuous media. Q. Appl. Math. 9, 381–389.

Faccio, P., Foraboschi, P., Siviero, E., 1999. Masonry vaults reinforced with FPR strips. L'Edilizia. 7, 44–50.

Fortunato, A., Fabbrocino, F., Angelillo, M., Fraternali, F., 2018. Limit analysis of masonry structures with free discontinuities. Meccanica 53, 1793–1802.

Foti, D., Vacca, V., Facchini, I., 2018. DEM modeling and experimental analysis of the static behavior of a dry-joints masonry cross vaults. Constr. Build. Mater. 170, 111–120.

Gaetani, A., Bianchini, N., Lourenço, P.B., 2020. Simplified micro-modelling of masonry cross vaults: stereotomy and interface issues. Int. J. Masonry Res. Innovat. 6 (1), 97–125.

Gobbin, F., De Felice, G., Lemos, J.V., 2020. A Discrete Element Model for masonry vaults strengthened with externally bonded reinforcement. Int. J. Archit. Herit. 1–14.

Grillanda, N., Chiozzi, A., Milani, G., Tralli, A., 2020. Efficient meta-heuristic mesh adaptation strategies for NURBS–based upper–bound limit analysis of general curved three-dimensional masonry structures. Comput. Struct. 236, 106271.

Hamid, A.A., Drysdale, R.G., 1988. Flexural tensile strength of concrete block masonry. J. Struct. Eng. 114, 50–66.

Heyman, J., 1966. The stone skeleton. Int. J. Solids Struct. 2, 249–256.

Heyman, J., 1969. The safety of masonry arches, Masonry Bridges. Viaducts Aqued. 11, 329–352.

Iannuzzo, A., Angelillo, M., De Chiara, E., De Guglielmo, F., De Serio, F., Ribera, F., Gesualdo, A., 2018. Modelling the cracks produced by settlements in masonry structures. Meccanica 53, 1857–1873.

Kennicott, P.R., 1996. Initial Graphics Exchange Specification, IGES 5.3, U.S. Product Data Association, North Charleston, South Carolina, USA.

Krejčí, T., Koudelka, T., Bernardo, V., Šejnoha, M., 2021. Effective elastic and fracture properties of regular and irregular masonry from nonlinear homogenization. Comput. Struct. 254, 106580.

Lemos, J.V., 2007. Discrete element modeling of masonry structures. Int. J. Architect. Herit. 1, 190–213.

Lubliner, J., Oliver, J., Oller, S., Oñate, E., 1989. A plastic-damage model for concrete. Int. J. Solids Struct. 25, 299–326.

Marmo, F., Masi, D., Mase, D., Rosati, L., 2019. Thrust network analysis of masonry vaults. Int. J. Masonry Res. Innovat. 4, 64–77.

Marmo, F., Rosati, L., 2017. Reformulation and extension of the thrust network analysis. Comput. Struct. 182, 104–118.

Milani, G., 2015. Upper bound sequential linear programming mesh adaptation scheme for collapse analysis of masonry vaults. Adv. Eng. Softw. 79, 91–110.

Milani, G., Bertolesi, E., 2017. Quasi-analytical homogenization approach for the non-linear analysis of in-plane loaded masonry panels. Constr. Build. Mater. 146, 723–743.

Milani, G., Lourenço, P.B., 2009. A discontinuous quasi-upper bound limit analysis approach with sequential linear programming mesh adaptation. Int. J. Mech. Sci. 51, 89–104.

Milani, E., Milani, G., Tralli, A., 2008. Limit analysis of masonry vaults by means of curved shell finite elements and homogenization. Int. J. Solids Struct. 45, 5258–5288.

Milani, G., Milani, E., Tralli, A., 2009. Upper bound limit analysis model for FRP – reinforced masonry curved structures. .Part II : Structural analyses. Comput. Struct. 87, 1534–1558.

Piegl, L., Tiller, W., 1995. The NURBS Book. Springer, Berlin.

Ponterosso, P., Fishwick, R., Fox, D.S., Liu, X., Begg, D., 2000. Masonry arch collapse loads and mechanisms by heuristically seeded genetic algorithm. Comput. Methods Appl. Mech. Eng. 190, 1233–1243.

Portioli, F., Casapulla, C., Gilbert, M., Cascini, L., 2014. Limit analysis of 3D masonry block structures with non-associative frictional joints using cone programming. Comput. Struct. 143, 108–121.

Portioli, F., Cascini, L., 2016. Assessment of masonry structures subjected to foundation settlements using rigid block limit analysis. Eng. Struct. 113, 347–361.

Portioli, F., Casapulla, C., Cascini, L., 2015. An efficient solution procedure for crushing failure in 3D limit analysis of masonry block structures with non-associative frictional joints. Int. J. Solids Struct. 69–70, 252–266.

Rekik, A., Gasser, A., 2016. Numerical homogenization model for effective creep properties of microcracked masonry. Int. J. Solids Struct. 102–103, 297–320.

Roca, P., Cervera, M., Gariup, G., Pelà, L., 2010. Structural analysis of masonry historical constructions. Classical and advanced approaches. Arch. Computat. Methods Eng. 17, 299–325.

Rossi, M., Calderini, C., Roselli, I., Mongeli, M., De Canio, G., Lagomarsino, S., 2020. Seismic analysis of a masonry cross vault through shaking table tests: the case study of the Dey Mosque in Algiers. Earthquakes Struct. 18, 57–72.

Sarhosis, V., Forgács, T., Lemos, J.V., 2019. A discrete approach for modelling backfill material in masonry arch bridges. Comput. Struct. 224, 106108.

Scacco, J., Milani, G., Lourenço, P.B., 2020. Automatic mesh generator for the non-linear homogenized analysis of double curvature masonry structures. Adv. Eng. Softw. 150, 102919.

Scacco, J., Ghiassi, B., Milani, G., Lourenço, P.B., 2020. A fast modeling approach for numerical analysis of unreinforced and FRCM reinforced masonry walls under out-of-plane loading. Compos. B Eng. 180, 107553.

Silva, L.C., Lourenço, P.B., Milani, G., 2017. Nonlinear discrete homogenized model for out-of-plane loaded masonry walls. J. Struct. Eng. 143, 04017099.

Wang, J., Melbourne, C., 1996. The 3-dimensional behaviour of skew masonry arches. The British Masonry Society, London, UK.

Zampieri, P., Cavalagli, N., Gusella, V., Pellegrino, C., 2018. Collapse displacements of masonry arch with geometrical uncertainties on spreading supports. Comput. Struct. 208, 118–129.

Zampieri, P., Simoncello, N., Pellegrino, C., 2018. Structural behaviour of masonry arch with no-horizontal springing settlement. Frattura Ed Integrita Strutturale. 14, 182–190.

Zampieri, P., Faleschini, F., Zanini, M.A., Simoncello, N., 2018. Collapse mechanisms of masonry arches with settled springing. Eng. Struct. 156, 363–374.

Zhang, Y., Macorini, L., Izzuddin, B.A., 2016. Mesoscale partitioned analysis of brick-masonry arches. Eng. Struct. 124, 142–166.